RSC Advances

Synthesis of Exfoliated Polystyrene/Anionic Clay MgAl-Layered double hydroxide: Structural and thermal properties

Amani M. Alansi[1], Waed Z Alkayali[1]; Maha H. Al-qunaibit[1]; Talal F. Qahtan[3]; Tawfik A. Saleh[2*],

[1] Chemistry Department, King Saud University, Saudi Arabia

[2] Chemistry Department, [3]Physics Department; King Fahd University of Petroleum & Minerals, Dhahran 31261, Saudi Arabia.

 *Corresponding Author tawfik@kfupm.edu.sa; tawfikas@hotmail.com

http://faculty.kfupm.edu.sa/CHEM/tawfik/publications.html

*Chemistry Department, King Fahd University of Petroleum & Minerals, Dhahran 31261, Saudi Arabia.

Abstract

Exfoliated polystyrene/layered double hydroxide (PS/LDH) nanocomposites were prepared by direct intercalation of PS into MgAl LDH at 60 °C. The MgAl LDH as nanofiller was modified via the precipitation of the salt mixture of magnesium and aluminum metals by sodium dodecyl sulfate (SDS). Various techniques, Fourier Transformed Infrared Spectroscopy (FTIR), X-Ray-diffraction (XRD), Filed Emission Transmission Electron Microscopy (FETE) and Thermo gravimetric analyses (TGA) were employed for structural properties and thermal stability of the nanocomposites. FTIR spectra indicated the presence of both functional groups of SDS-LDH and PS. XRD patterns and TEM images indicated the formation of amorphous dispersed and exfoliated nanocomposites. Increase in thermal stability with SDS-MgAl LDH content was observed by TGA and DTG through the $T_{0.5}$ ($T_{0.5}$ the degradation temperature at 50%) and T_{max} (T_{max} the maximum rate of change) with a maximum obtained for a loading of 2 and 4 wt%.

Keywords: *polystyrene, layered double hydroxides, direct intercalation, nanocomposites, rapid precipitation, thermal stability.*

1. Introduction

Nowadays, the applications of the various polymer nancomposites in many industrial fields have become more important and given a precious opportunity to develop new nanocomposite formats with improved properties compared to composites made with traditional materials. There has been a growing interest in using nanostructured materials. Recently, layered double hydroxides (LDHs), famous as anionic clay, have become a new promising nanostructured material used as nanofiller to obtain polymer nanocomposites. LDHs are inorganic materials that consist of metal layered/layered double hydroxides and hydroxide sheets with different intercalated anions and

some water molecules.[1, 2] The general formula of LDHs is defined as $[M^{2+}_{1-x} M^{3+}_x (OH)_2]^{x+}$. $A^{n-}_{x/n}.zH_2O$, is (LDH) with M^{2+} and M^{3+} : divalent and trivalent metal cations such as Mg^{2+}, Ca^{2+}, Zn^{2+}, Ni^{2+}, Mn^{2+}, Al^{3+}, Co^{3+}, Fe^{3+}, V^{3+}, and A is a charge-balancing interlayer anion such as CO_3^{-2}, NO_3^- Cl^-. The value of x usually can exist in the range of (0.2 - 0.3).[3, 4] Mg–Al LDH with formula $[Mg^{2+}_{1-x}Al^{3+}_x(OH)_2](A^{n-})_{x/n}.mH_2O)$ is an anionic clay mineral exhibiting an anion exchange property. The host lattice of the layer-structured crystal consists of brucite $(Mg(OH)_2)$-like octahedral layers which are positively charged. The positive charges of the host lattice are neutralized by the intercalated anions in the interlayers, and its remaining space is occupied by water molecules.[5] LDHs have attracted considerable interest due to their beneficial applications in various fields like catalysis, catalyst support, ion-exchange, adsorbents, environmental, photochemistry, electrochemistry, biochemistry, medicine, polymer additives and heat stabilizers.[6-8]

Original LDHs are not suitable to synthesize the polymer nanocomposites. This is because LDHs are hydrophilic materials and have very small interlayer spacing, which makes the intercalation of organic polymer molecules practically impossible. Therefore, modification of LDHs by insertion of organic anion species is necessary. The organic anion species can decrease the hydrophilic feature and increase the interlayer distance of LDHs and this can improve the compatibility between LDHs and polymer matrix. The modification by organic anions includes many anions such as the salts of carboxylates, sulfonates, sulfates and phosphates.[9, 10]

LDHs that used as a nanofiller for the preparation polymer nanocomposites can enhance many properties of the intended polymers such as, gas barrier,[11, 12] flame-retardancy,[13] and mechanical and thermal properties. [14-17] which are not present in conventional composites or pure polymer. Polystyrene is one of the types of thermoplastics that are widely used in applications at low

cost.[18] The thermal stability of polymers plays a major role in determining their suitability for applications in various fields such as engineering, construction and food packaging. This property could be improved by adding thermally stable inorganic materials such as metals,[19] metal oxides[18] and LDHs into polymer.[20-22]

Polymer/ LDHs nanocomposites were reported to be prepared by the intercalation of monomer molecules into clay layers, followed by the in-situ polymerization process[23-25] or by the direct intercalation of polymer chain into LDH layers.[3, 21, 22] Many types of the polymer/LDH nanocomposites were reported.[26-29]

Efforts have been made for improving the physical and mechanical properties and processability of PS.[30, 31] To overcome these limitations, copolymerization of styrene and another monomer, the postfunctionalization of PS via sulfonation or Friedel–Crafts acylation reactions, and graft copolymerization were investigated.[32-34] Nanocomposite of exfoliated PS/ZnAl LDH was developed via emulsion polymerization. The thermal decomposition of nanocomposites with 5% wt of LDH was reported to be higher than that of neat polystyrene.[35] Exfoliated ZnAl LDH /PS nanocomposites were prepared from initiator-modified ZnAl LDH as filler in PS via in-situ atom transfer radical polymerization process.[36] Nanocomposite of ammonium polyphosphate modified MgAl LDH polystyrene was reported to increase the flame resistance.[4] The heterocoagulation process was employed for the preparation of polystyrene/LDH composite with improved thermal stability as a result of the well dispersion of LDHs within PS matrix.[37] PS nanocomposites using different kinds of LDHs organo-modified were prepared by solvent blending process.[22] However, the previous studies reported on synthesis methods are either complex or expensive for obtaining the exfoliated nanocomposites. The originality of this study is indeed the introduction of simple and inexpensive synthesis method of exfoliated PS/MgAl-LDH nanocomposites. It consists of a

direct intercalation of PS in SDS-LDH under reflux in toluene solution at low temperature (60 °C) and in the presence of ethanol to reduce the agglomeration. In the present case, we have got a great exfoliation in the synthesized nanocomposites and a clear increase in thermal stability. MgAl- LDHs have been modified by using sodium dodecyl sulfate (SDS) as an organic anion to enhance the compatibility between the LDH layers and the polymer matrix.

2. Experimental Section

2.1. Materials

Polystyrene (Mw = 259,000 g/mol) was provided by the Saudi Basic Industries Corporation (SABIC) and the trade name as PS125. $Mg(NO_3)_2.6H_2O$ was received from LOBA, $Al(NO_3)_3.9H_2O$, NaOH and ethanol from BDH , Sodium Dodecyl Sulfate (SDS) ($NaC_{12}H_{25}SO_4$ Mw = 288.38 g/mol) from WINLAB and toluene from AVONCHEM . All the last materials have been purchased from Saudi Arabia

2.2. Preparation of (MgAl-LDH)

Co-precipitation method was used to synthesize MgAl-LDH.[38] A mixture of magnesium nitrate (0.75 M) $Mg(NO_3)_2.6H_2O$ and aluminum nitrate (0.25 M) $Al(NO_3)_3.9H_2O$ was added into deionized water (120 mL). The mixture was slowly dropped (flow rate: 0.20 mL per min) into 120 mL of sodium hydroxide solution (1M) with constant stirring and heating (70 °C). The pH value was kept at 9 by adding NaOH solution (1M). The obtained precipitate was aged under the same conditions for 24 h. Then, it was filtered, washed several times using deionized water and dried in an oven at 60 °C for 1 day.

2.3. Preparation of (SDS-MgAl-LDH)

A mixture of magnesium nitrate (0.75 M) $Mg(NO_3)_2.6H_2O$ and aluminum nitrate (0.25 M) $Al(NO_3)_3.9H_2O$ was added into deionized water (120 mL). The mixture was slowly dropped (flow rate: 0.20 mL per min) into 120 mL of sodium dodecyl sulfate (0.6 M) with constant stirring and heating (70 ^{o}C). The pH value was kept at 9 by adding NaOH solution (1M). The obtained precipitate was aged under the same conditions for 24 h. Then, it was filtered, washed several times using deionized water and dried in an oven at 60 ^{o}C for 1 day.

2.4. Preparation of PS/SDS-MgAl-LDH nanocomposites

The direct intercalation process was employed to synthesize the PS/SDS-MgAl-LDH nanocomposites. A certain amount of SDS-MgAl LDH was refluxed in 10 mL toluene for 24 h at room temperature. Then, 10 mL PS was added to the suspended solution of SDS-MgAl LDH and the mixture was refluxed for 3 h at 60 ^{o}C then added into 100 mL ethanol for fast precipitation. After filtering, the synthesized precipitate was dried for 48h at 100 ^{o}C. The nanocomposite samples were prepared with different loadings. We studied the range between 0.5 and 4 wt % of SDS-MgAl LDH. PS solution was prepared by dissolving granules of PS in toluene at room temperature.

2.5. Characterization

The crystalline structures of prepared samples were obtained by X-ray diffraction using a Rigaku Miniflex II diffractometer with Cu radiation (30 kV, 15 mA) equipped with Ni-filtered and the scanning speed was 2.0 $^{\circ}$/min. Fourier Transformed transform infrared (FTIR) spectra for the synthesized samples were recorded by FTIR spectrometer 1000, and Perkin Elmer using dry KBr as a standard reference in the range of 400–4000 cm^{-1}. The morphology of the obtained samples and the dispersion morphology of SDS-LDH in PS matrix were characterized using (

JEOL JEM-2100F), and an advanced Field Emission Electron Microscope operated (FETEM) with an accelerating voltage of 200 KV. The thermodegradation of prepared samples was evaluated via thermo gravimetric analysis (TGA) with a Perkin-Elmer analyzer. A thermogram, was determined from 25 $^{\circ}$C to 800 $^{\circ}$C at a heating rate of 10 $^{\circ}$C min^{-1} under nitrogen flow.

3. Results and Discussion

3.1. Structural characterization of PS/Mg-Al LDH nanocomposites

FTIR Spectra: The FT-IR spectra of LDH, SDS- LDH, PS/ (4, 2, 1 and 0.5,) wt.% SDS-LDH nanocomposites and pure PS, have been shown in Fig. 1. The FT-IR spectrum of MgAl LDH indicated characteristic absorption bands. First to start with is the broad band at around 3200–3600 cm^{-1} region (maximum at 3528 cm^{-1} and 3480 cm^{-1} for LDH-SDS and LDH respectively,) could be assigned to the symmetric and asymmetric stretching mode of hydrogen-bonded hydroxyle groups in the hydroxyl layers (Mg/Al–OH or Al–OH) of LDH and the interlayer water molecules or to lattice water.[39] The corresponding bending OH vibration mode of water molecules appears around 1624 cm^{-1} and 1635 cm^{-1} for LDH and SDS-LDH respectivly, Table 1. Lattice vibration bands, observed in the 800–400 cm^{-1} region are assigned to Mg–O, Al–O, O–Al–O or O–Al–O modes.[40, 41] The absence of the NO_3^- bands at about 1384 cm^{-1} in the spectra of the SDS- LDH could be an indication of the completeness of the exchange process.[4] The absorption bands at approximately 2920 and 2850 cm^{-1} are ascribed to the stretching vibration of CH_2 and CH_3 found in SDS. The band approximatlly 1468 cm^{-1} can be assigned to C–H bending vibration.[42, 43] Peaks observed at about 1210 and 1062 cm^{-1}, could be assigned to symmetric and asymmetric stretching vibrations of bands of sulfate (SO_4^{2-}) groups which confirm the presence of SDS.

7

The FT-IR spectra of pure PS show the characteristic absorption bands at 2924 and 2857 cm^{-1} due to the symmetric and asymmetric stretching vibration of C–H; at 1601 and 1510cm^{-1} due to the C=C stretching vibrations; at 1445 and 1372cm^{-1}, assigned to –CH_2 bending vibrations and (C–H) in the aromatic ring at 700 and 750 cm^{-1}.[28, 19, 18]

The FTIR spectra of PS/SDS-MgAl LDH samples with 4, 2, 1 and 0.5 wt% SDS-LDH reveal the combination of spectra SDS-LDH and pure PS. The peaks recorded at around (3416.6- 3415 cm^{-1}) and (1617.8- 1619.2 cm^{-1}) are attributable to OH stretching modes and H_2O bending modes. The absorption bands of the lattice vibration modes assigned to Mg–O, Al–O, O–Al–O or O–Al–O modes in the 800-400 cm^{-1} region which provides evidence that SDS-LDH layers were dispersed in the PS matrix.[37]

Table .1. The FTIR spectra of SDS-LDH and PS/ (4, 2, 1 and 0.5) wt. % SDS-MgAl-LDH nanocomposites.

Assignment	SDS-LDH	PS/0.5% wt SDS-LDH (cm^{-1})	PS/1% wt SDS-LDH (cm^{-1})	PS/2% wt SDS-LDH (cm^{-1})	PS/4% wt SDS-LDH (cm^{-1})
(OH) stretching modes	3528	3416.6	3416.1	3415.7	3415.41
(H_2O) bending motion	1635	1617.8	1618.30	1618.95	1619.23
(M-O and O-M-O) vibration modes			800-400		
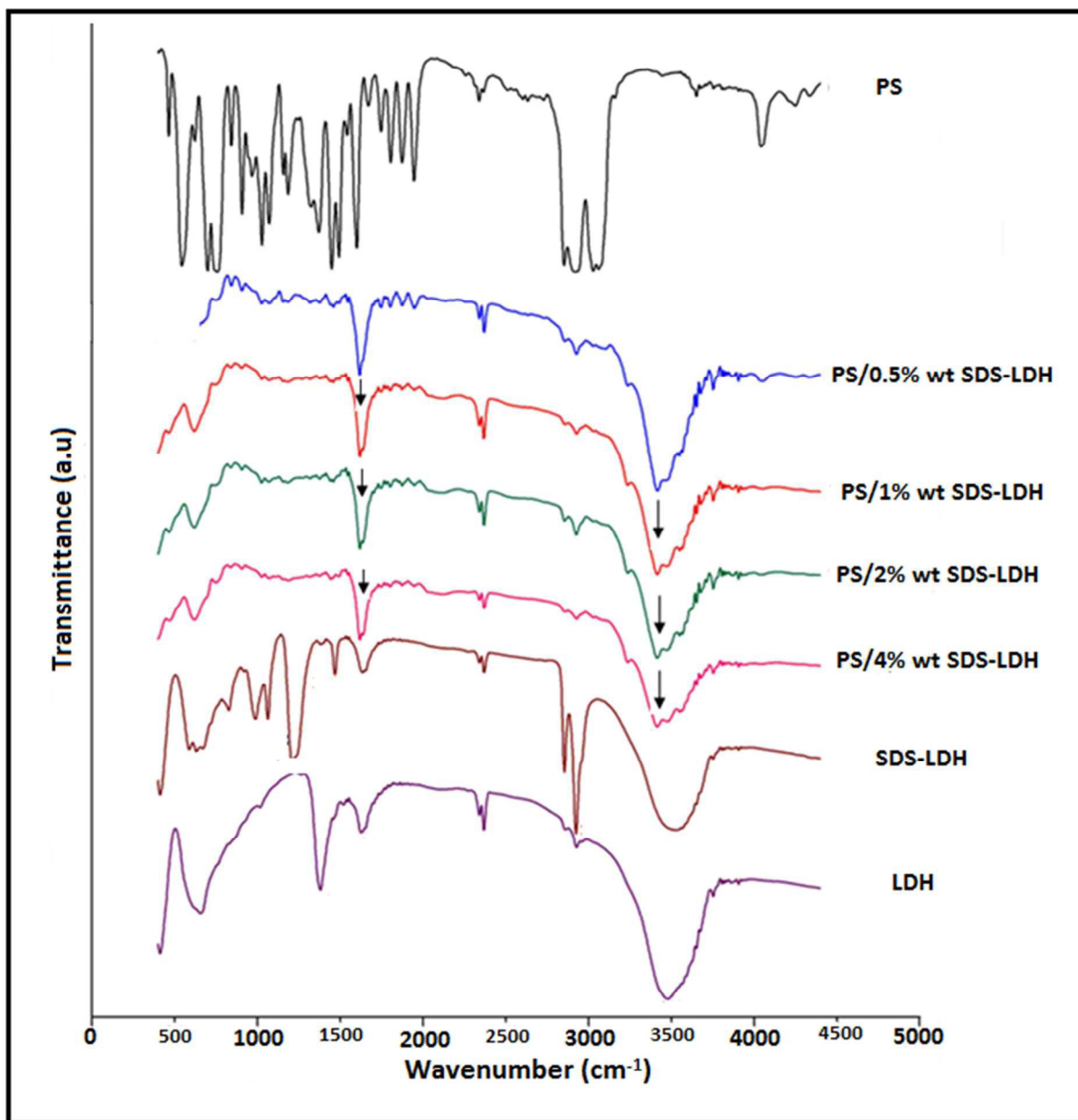
Fig.1. FTIR spectra of LDH, SDS-LDH, PS/ (4, 2, 1 and 0.5) wt. % SDS-MgAl-LDH nanocomposites and pure PS.

X-Ray Diffraction: In nanocomposites, the XRD is an important characterization mean to describe the types of the layered structure formed in intercalated and/or exfoliated polymer/LDH.

9

The intercalated structure is formed when the d-spacing between LDH layers increases to a few nanometers. Whereas in the case of exfoliated structure, it is formed when the LDH layers totally lose their regular crystalline structure and move away from each other. The degree of exfoliation or the presence of a small diffracting volume can be detected by the disappearance of XRD peaks. The exfoliation state can be detected by direct observation by TEM.

The X-ray diffraction (XRD) patterns of LDH, SDS- LDH and PS (4, 1, 2, 0.5,) wt% of SDS-LDH and pure PS are depicted in Fig.2. The basal peak positions indicate the interlayer spacing between two metal hydroxide sheets. The basal reflection of LDH and SDS-LDH were located at $2\theta = 11.4°$ and $3.03°$ respectively. One can notice the presence of a shift by $8.37°$ which is attributed to the expansion of the interlayer spacing of LDH. The interlayer spacing corresponding to these peaks is 0.78 and 2.90 nm, respectively.[44-46] This could confirm that SDS-anion has been inserted between LDH layers.

From the XRD patterns of the nanocomposites containing 4, 2, 1, 0.5 % wt of SDS-LDH, it is clear that the basal peak (around $3°$) of SDS-LDH disappeared. This can be explained by the complete covering of LDH by PS chains. However, the presence of SDS-LDH is supported by the two diffraction peaks ($2\theta = 10°$, $20°$) for pure PS which exist in all the nanocomposites.[45, 47] Thus, these diffraction patterns suggest that the SDS-MgAl-LDH layers may be exfoliated in the polystyrene matrix and confirmed that the PS/SDS- MgAl-LDH nanocomposites were formed successfully via direct intercalation at low temperature and rapid precipitation process. These results revealed the structural changes with loading SDS-LDH. It should be noted that the exfoliation state could be detected by direct observation of TEM images as is discussed in the following sections.
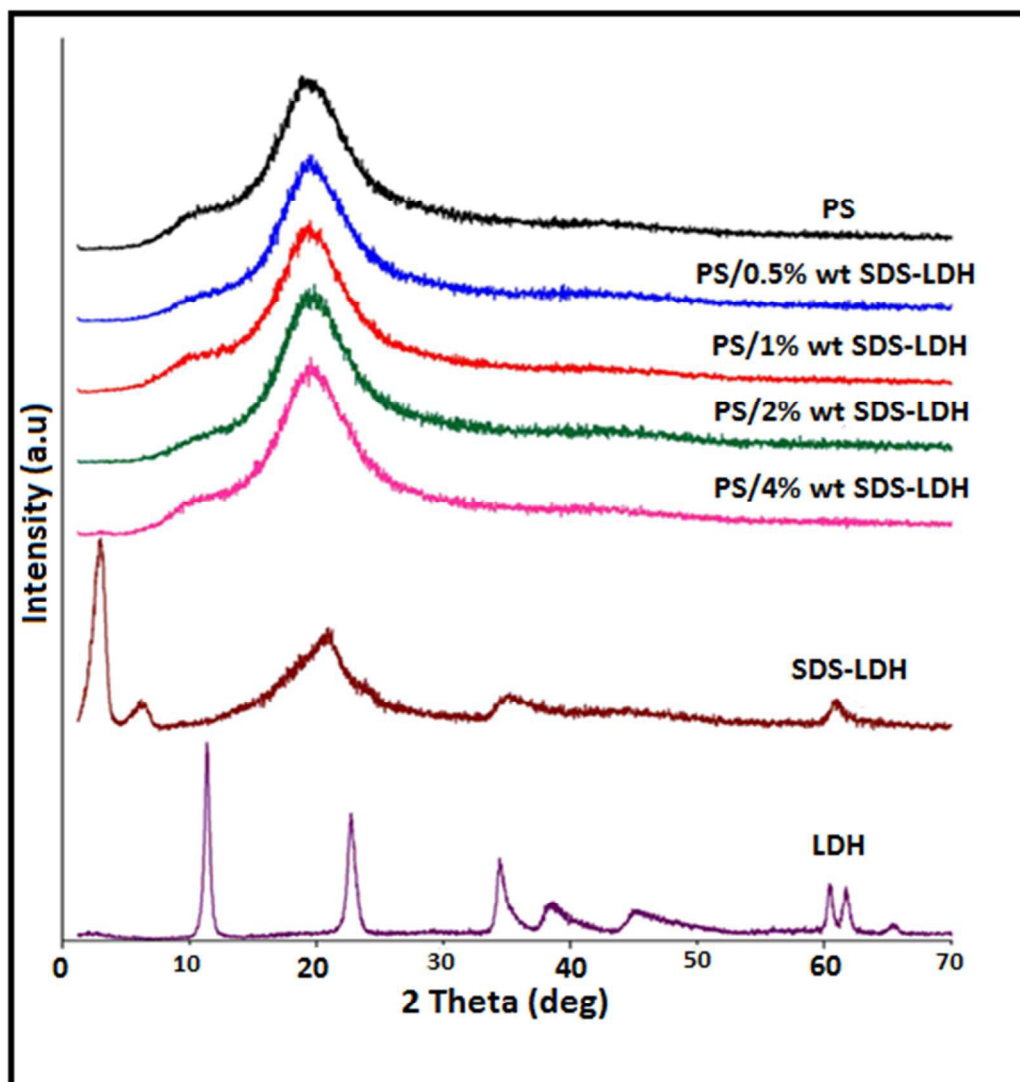
Fig.2. X-ray diffraction data of: LDH, SDS-LDH, PS/ (4, 2, 1 and 0.5) wt. % SDS-LDH nanocomposites and pure PS.

Morphological structures of PS /MgAl LDH nanocomposites

Microscopic analysis is necessary to show the distribution and dispersion of LDH layers in the polymer matrix. A TEM image can determine whether the type of structure formed is intercalated, exfoliated or both together. Fig.3-a. depicts the TEM images of LDH which show many thin platelets stacked orderly and tightly on top of each other by the strong attractive force

among the interlayer anions with a particle size of 100 nm. This result was ascribed to homogeneous and slow precipitation of LDH. As shown in Fig.3-b there are many thin platelets of SDS-LDH which are less orderly stacked on top of each other with a particle size of 100 nm. This result suggests the SDS intercalated into the nanolayers of LDH agreed with XRD analysis.
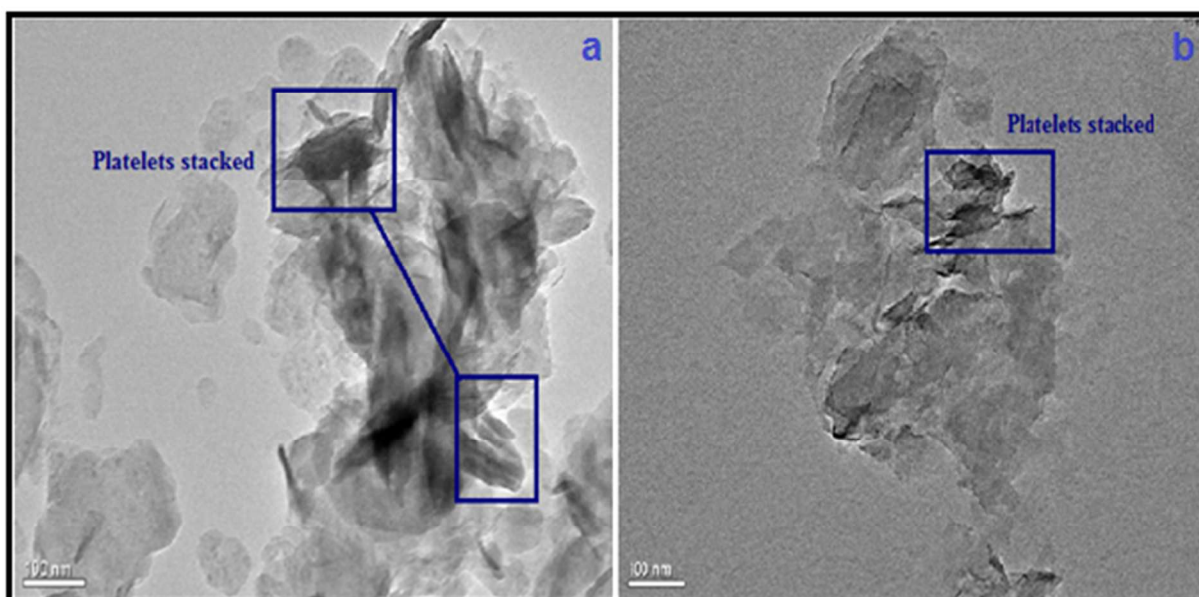
Fig.3. TEM analysis of (a) MgAl LDH and (b) SDS- MgAl LDH.

The TEM images of PS/SDS-LDH nanocomposites with 0.5, 1, 2, and 4 wt% of SDS-LDH are depicted in Figs.4-a, b, c and d respectively in various nano-scale size. The dark lines correspond to the modified- LDH layers, whereas the gray regions represent the polystyrene matrix. As shown in (0.5, 1, 2 and 4 wt %) nanocomposite samples shown in Fig.4-a, b, c and d , the ordered layered structure of many modified-LDH nanolayers was totally lost and exfoliated in PS matrix with few intercalated nanolayers . The exfoliated of SDS-LDH into individual layers can be clearly seen in the filler particle region. These results confirmed all nanocomposite

samples were disorderly dispersed and exfoliated into the PS matrix with some aggregated regions, which is in a good agreement with previous studies.[46, 48] Therefore, TEM results confirmed the results of XRD patterns, where the images of TEM showed that all nanocomposite samples prepared by this method were disorderly dispersed and exfoliated into the PS matrix.

Fig.5. depicts the schematic diagram of the synthesis mechanism of the MgAl LDH, SDS-MgAl LDH via co-precipitation method and PS/SDS-MgAl-LDH nanocomposites via direct intercalation method depending on the obtained results from XRD and TEM.
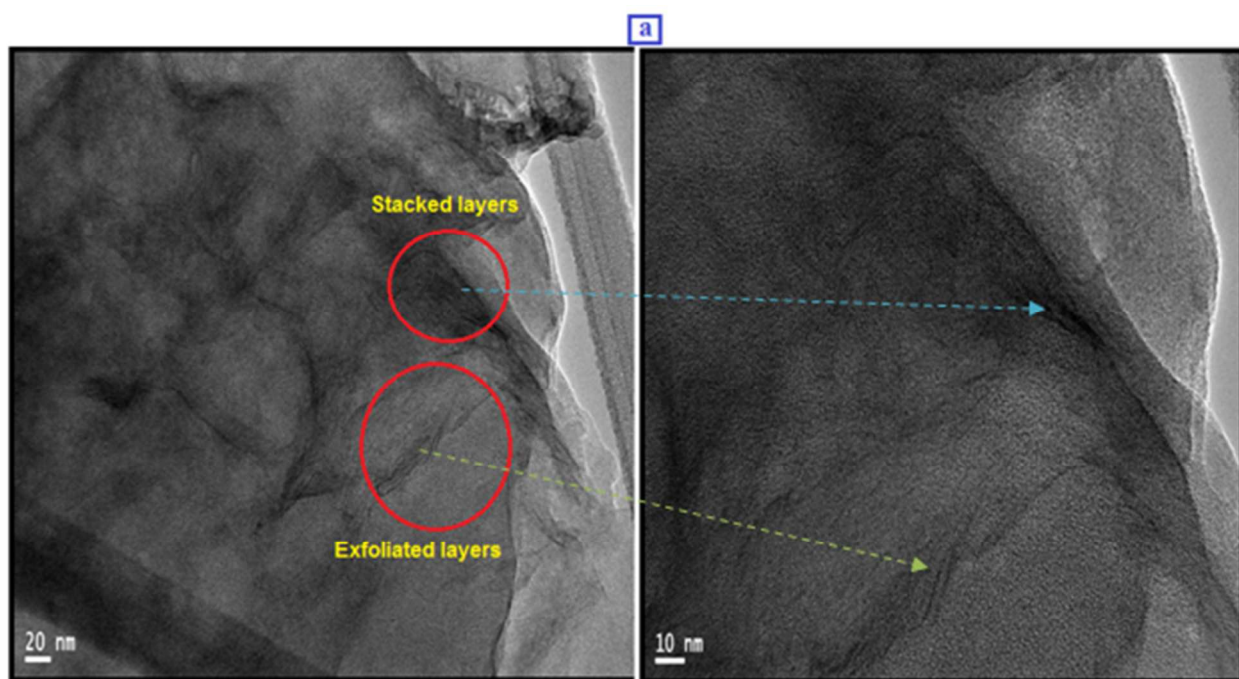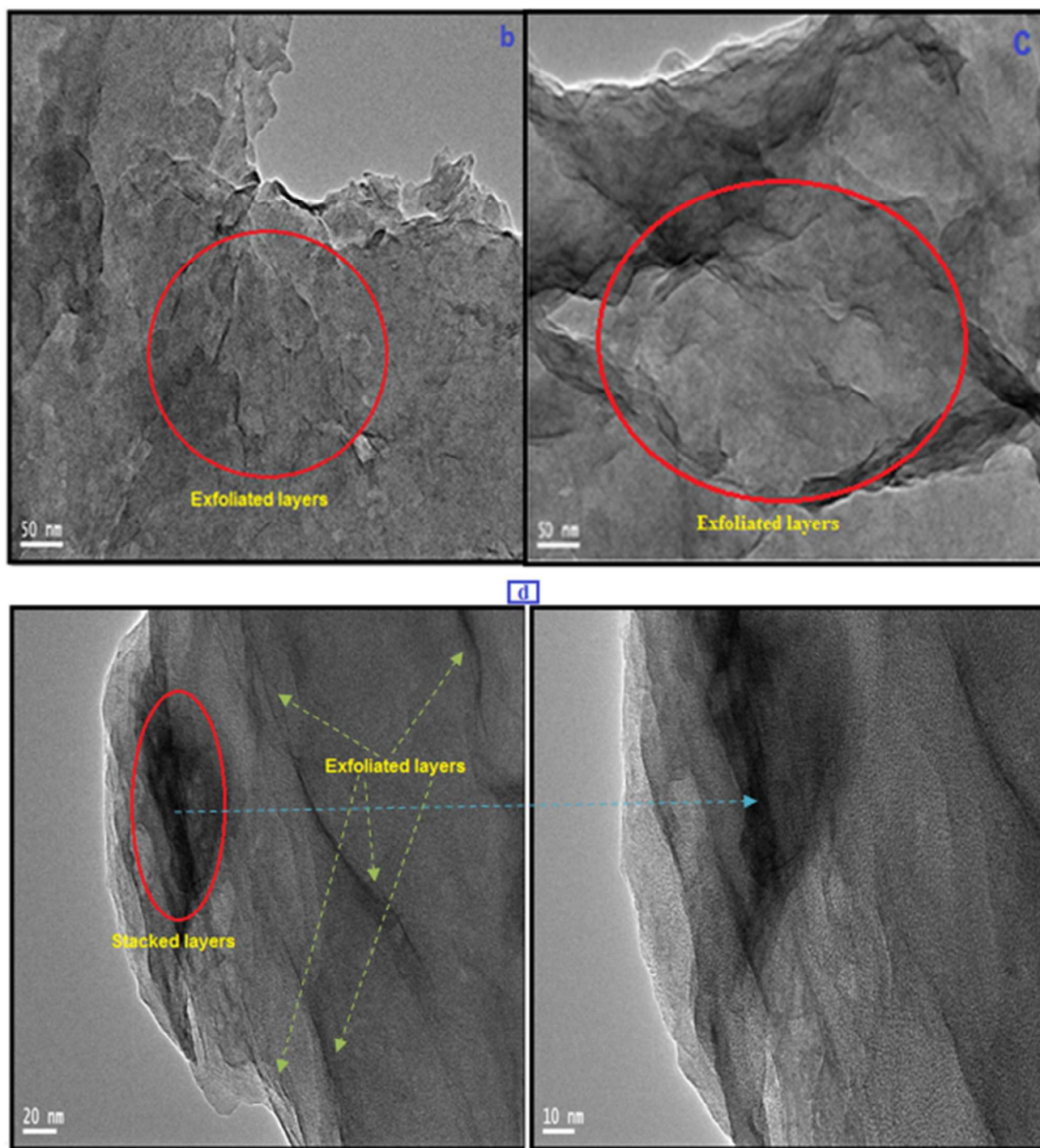
Fig.4. TEM images of different contents of (SDS-MgAl LDH) in the PS/LDH nanocomposite samples: (a) 0.5 wt%, (b) 1 wt%, (c) 2 wt% and 4 wt%.
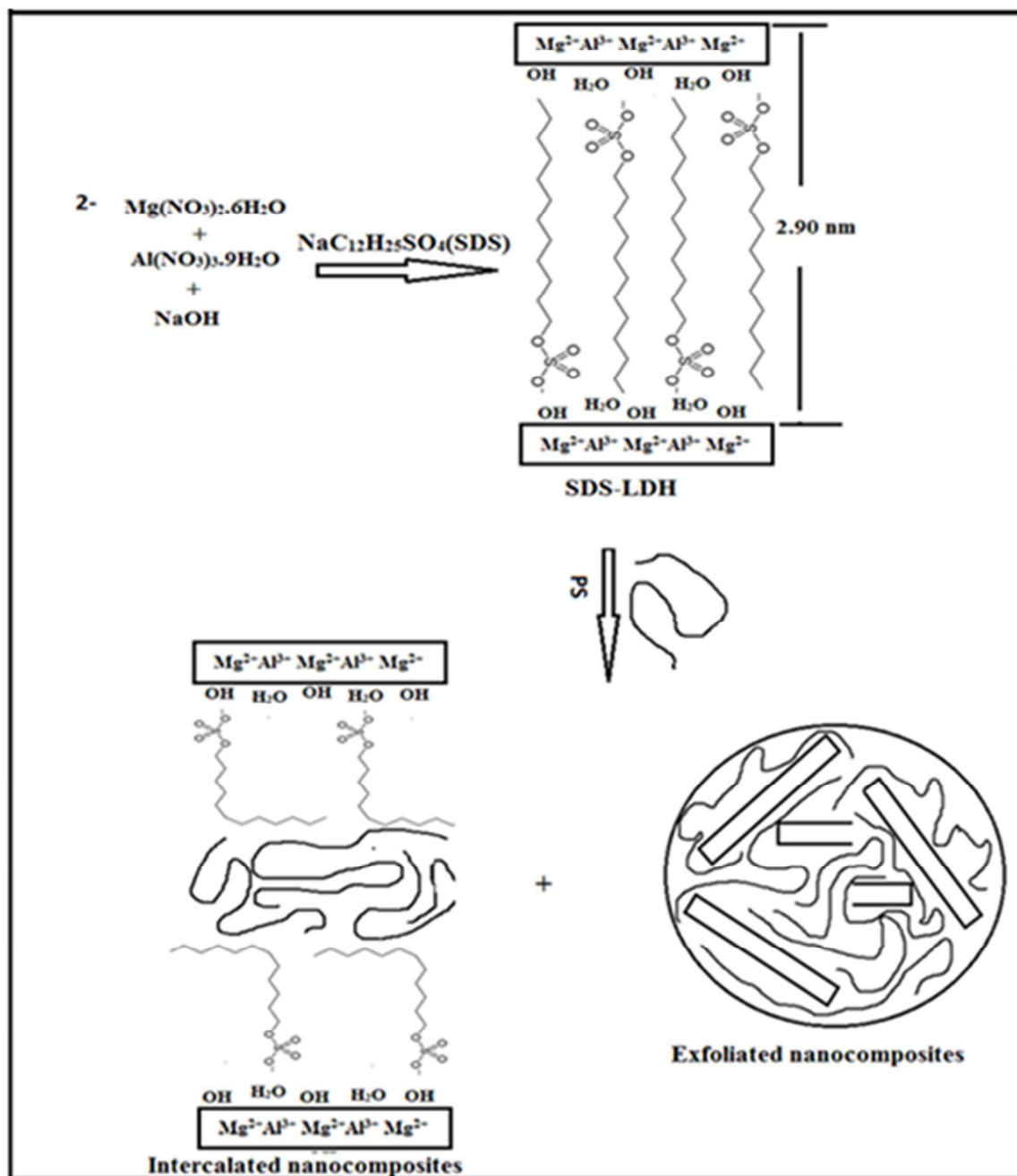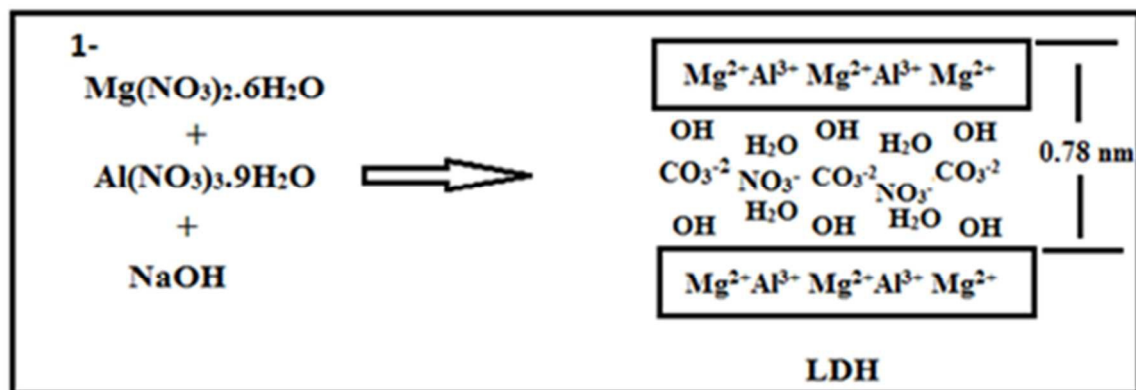
Fig.5. Scheme of steps involved in the preparation of MgAl LDH, SDS-MgAl LDH, and PS/SDS-MgAl LDH nanocomposites.

Thermal characterization of PS/Mg-Al LDH nanocomposites

The thermal stability of MgAl LDH and modified-MgAl LDH was depicted by TGA curves in Fig.6. From these curve, the decomposition of LDH was divided into three stages.[49, 50] The first stage is from room temperature up to 220 $^{\circ}$C which is due to the loss of physically adsorbed and interlayer water. The second stage is from 296 to 500 $^{\circ}$C which is attributed to the dehydroxylation of the LDH layer and carbonate loss. The third stage began at 500 and ended at 760 $^{\circ}$C that resulted from the decomposition of the mixed metal oxides.[35] The total mass loss of LDH in the region 25–760 $^{\circ}$C was 43.23 %. The degradation of modified-MgAl LDH was divided into four stages. The first one below 120 $^{\circ}$C is due to the loss of adsorbed and interlayer water. The second stage from 1 89to 260 $^{\circ}$C can be attributed to the decomposition of SDS chain in the LDH layer. However, the third stage around 270 to 510 $^{\circ}$C is because of the dehydroxylation of the LDH layers. The decomposition temperature of dehydroxylation was increased because of the hindrance resulting from the decomposition of the SDS chain. The fourth stage begins at 550 and ended at 780 $^{\circ}$C and it is proposed that this could be the result of the decomposition of the mixed metal oxides. The total mass loss of SDS-LDH for the region (25–780 $^{\circ}$C) was 68.09%. The second stage of SDS-LDH was assigned to the presence of organic anion SDS in LDH.[51] The results of the thermal decomposition of LDH and modified LDH illustrated the extent of the thermal stability of these materials. The TGA results were in agreement with results reported in the literature.[38, 46, 52-55]

16
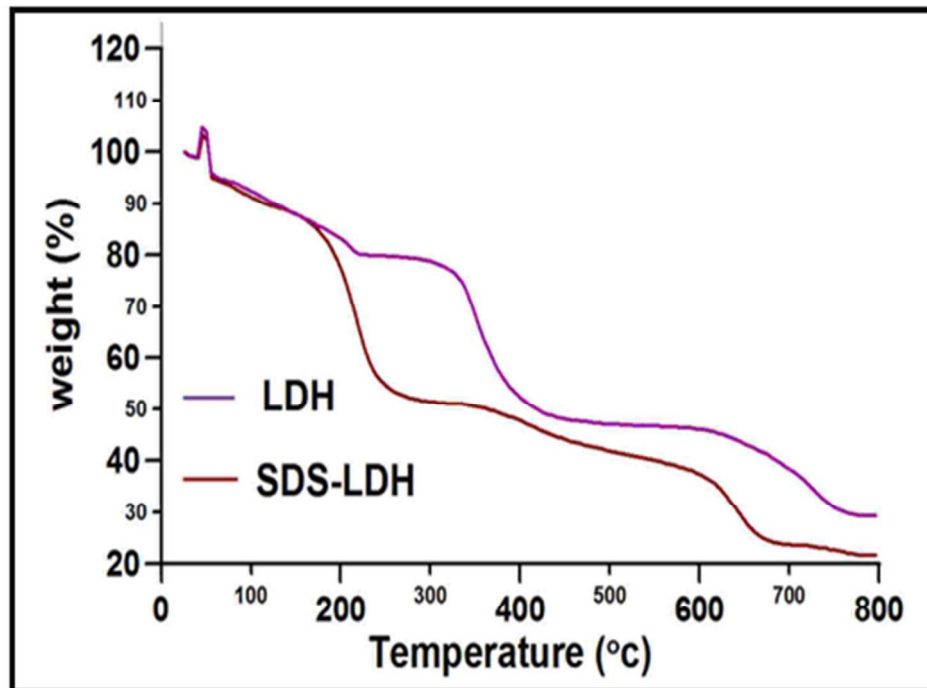
Fig.6. TGA thermograms of MgAl LDH and SDS- MgAl LDH.

The thermal stability of the prepared polymeric composites have been investigated. The thermal stability of nanocomposites and pure PS was compared using TGA and DTG analysis. Fig. S1. (Supplementary file) depicts the TGA mass loss curves and corresponding derivative curves (DTG) of the PS/ modified LDH samples and the pure PS. From TGA curve, the thermal decomposition of the pure PS occurred in the range of 200-450 ^{o}C which was attributed the decomposition of the polymer backbone of PS. However, it is clear from the TGA curve of PS that there is a slight decomposition occurred before 200 ^{o}C. This decomposition may be due to the evaporation of the solvent.

The presence of SDS-LDH in the nanocomposite samples causes simple changes in the thermal degradation behavior in comparison to pure PS. From TGA curves, the thermal degradation of the PS/SDS-LDH nanocomposites divided into two stages. The first decomposition stage occurs

at about (100-200 $^{\circ}$C). This decomposition stage is attributed to the evaporation of adsorbed water on SDS-LDH layers which agreement with FTIR. The second decomposition step takes place at the temperature range of (250-460 $^{\circ}$C). This step is due to the thermal decomposition of PS, SDS alkyl chains and the formation of black charred residues. Clearly, TGA curves showed that the decomposition rate of the nanocomposite samples is lower than the one for PS, and this is due to the physical interactions between the polymer and layers of LDH. With these interactions, the material presents a higher resistance to diffusion of oxygen and volatile compounds, contributing to slower degradation.[45]

Generally, the TGA curves of PS/SDS-LDH $T_{0.5}$ (degradation temperature at 50% of weight) from TGA curves and T_{max} (the maximum rate of change) from (DTG) were chosen as the points of comparison. The thermal degradation temperatures ($T_{0.5}$) for pure PS and the nanocomposites containing 0.5, 1, 2 and 4 wt% modified-LDH were determined to be 398, 398, 400, 407 and 407 $^{\circ}$C, respectively. Also, (T_{max}) the maximum rate of change of the curve (DTG) of unfilled PS and the nanocomposites containing 0.5, 1, 2 and 4 wt% modified-LDH appeared at 404, 407, 406, 413 and 413 $^{\circ}$C, respectively. Nanocomposites in all compositions showed higher degradation temperatures than obtained for the pure PS. It is clear that, the thermal stability of the nanocomposite samples was increased with increasing the amount of SDS-LDH. In addition, the residues of the nanocomposites were increased with the increase in the amount of modified-LDH as was clear from TGA curves. TGA results indicated that the enhancement in the thermal stability of the nanocomposites was ascribed to the homogeneous dispersion of SDS-LDH in the PS and to the increase in the modified LDH content that could act as a superficial framework and as a mass transport barrier between the layers.

4. Conclusion

The synthesis of exfoliated polystyrene (PS) /modified MgAl layered double hydroxide (SDS-MgAl LDH) nanocomposites was achieved by excellent direct intercalation and a rapid precipitation process under reflux in toluene at low temperature 60 ^{o}C. XRD and FTIR analysis confirmed that the SDS anion intercalated into the interlayers of MgAl LDH at 70 ^{o}C. The XRD pattern showed an increase in the interlayer distance of the modified LDH from 0.78 nm to 2.90 nm with the intercalated SDS anion. XRD patterns and TEM images indicated the formation of exfoliated PS /modified-MgAl LDH nanocomposites. The enhancement in the thermal stability of the modified composites was proved by TGA and DTG through the $T_{0.5}$ and T_{max}, respectively, with a maximum obtained for a loading of 2 and 4 wt% SDS- MgAl LDH. The enhancement in the thermal stability of the nanocomposites could be ascribed to the amorphous dispersion of SDS-LDH in the PS and the increase in the modified LDH content as observed by TEM, XRD and TGA.

ACKNOWLEDGEMENTS

REFERENCES

1. C. D. Hoyo, *Appl. Clay Sci.,* 2007, **36**, 103–121.
2. Y. You, H. Zhao and G. F. Vance, *J. Mater. Chem*., 2002, **12**, 907-912.

3.   H. Acharya, S. K. Srivastava, and A. K. Bhowmick, Compo. *Sci. Technol.*, 2007, **67**, 2807-2811.
4.   C. Nyambo, E. Kandare, J. Wang and C. A. Wilkie, *Polym. Degrad. Stab.*, 2008, **93**, 1656-1660.
5.   T. Kameda, M. Saito and Y. Umetsu, *Mater. Trans.*, 2006, **47**, 923 – 930.
6.   S. Bhattacharjee and J. A. Anderson, *Chem. Commun.*, 2004, **5**, 554-555.
7.   Z.A. Jamiu, T.A. Saleh, S.A. Ali, *RSC Advances*, 2015, 5, 42222-42232.
8.   V.K Gupta, I Ali , T.A. Saleh , A. Nayak and S. Agarwal., *RSC Advances*, 2012, 2, 6380–6388.
9.   P. Ding and B. Qu, J. Polym. Sci. Part B: *Polym. Phys.*, 2006, **44**, 3165–3172.
10.   T. Kuila, H. Acharya, S. K. Srivastava and A. K. Bhowmick, *J. Appl. Polym. Sci.*, 2008, **108**, 1329–1335.
11.   P. B. Messersmith and E. P. Giannelis, *Chem. Mater.,* 1994, **6**, 1719-1725.
12.   Y. Kojima, A. Fujushima, A., Usuki, A. Okada and T. J. Kurauchi, *J. Mate. Sci. Lett.*, 1993, **12**, 889-890.
13.   J. W. Gilman, T. Kashiwagi and J. D. Lichtenhan, *SAMPE. J.*, 1997, **33**, 40-46.
14.   E. P. Giannelis, *Adv. Mate.*, 1996, **8**, 29-35.
15.   A. Usuki, Y. Kojima, M. Kawasumi, A. Okada, A. Fu-Jushima, T. Kurauchi and O. Kamigaito, *J. Mater. Res.*, 1993, **8**, 1179-1184.
16.   Y. Kojima, A. Usuki, M. Kawasumi, A. Okada, A. Fu-Jushima, T. Kurauchi and O. Kamigaito, *J. Mater. Res*., 1993, **8**, 1185-1189.
17.   T. Lan, T. J. Pinnavaia, *Chem. of Mate.*, 1994, **6**, 2216-2219.
18.   X. Yan, Q. He, X. Zhang, H. Gu, H. Chen, Q. Wang, L. Sun, S. Wei and Z. Guo, *Macromol. Mater. Eng*., 2014, **299**, 485-494.
19.   X. Chen, S. Wei, C. Gunesoglu, J. Zhu, C. S. Southworth, L. Sun, A. B. Karki, D.P. Young and Z. Guo, *Macromol. Chem. Phys*., 2010, **211**, 1775-1783.
20.   W. Chen, L. Feng and B. Qu, *Chem. Mater*., 2004, **16**, 368 – 370.
21.   C. S. Liao and W. B. Ye, *J. Polym. Res*., 2003, **10** ,241 – 246.
22.   B. Sahu and G. Pugazhenthi, *J. Appl. Polym. Sci*, 2011, **120** ,2485–2495.
23.   M. Tanaka, I. Y. Park, K. Kuroda and C. Kato, *Bull. Chem. Soc. Jpn*., 1989, **62,** 3442-3445.
24.   V. P. Isupov, L. E. Chupakhina, M.A. Ozerova, V. G. Kostrovsky and V. A. Poluboyarov, *Solid States Ionics*, 2001, **41-142**, 231 – 236.
25.   C. Berti, M. Fiorini and L. Sisti, Eur. *Polym. J.,* 2009, **45** ,70–78.
26.   W. Chen and B. Qu B, *Chem. Mater*., 2003, **15**, 3208-3213.
27.   E. M. Moujahid, J. P. Besse and F. Leroux, *J. Mater. Chem*., 2002, **12**, 3324-3328.
28.   Y. Gao, Q. Wang, J. Wang, L. Huang, X. Yan, X. Zhang, Q. He, Z. Xing and Z. Guo, *ACS Applied Materials & Interfaces*, 2014, **6**, 5094-5104.
29.   Q. Wang, J. Wu, Y. Gao, Z. Zhang, J. Wang, X. Zhang, X. Yan, A. Umar, Z. Guob and D. O'Hare, *RSC Advances*, 2013, **3**, 26017-26024.
30.   Y. Gao, S. Li, H. Li and X. Wang, *Eur. Polym. J.,* 2005, **41**, 2329–2334.
31.   Y. Gao and H. M. Li, *Polym. Int*., 2004, **53**, 1436–1441.
32.   J. Shin, M. S. Jensen, J. Ju, S. Lee, Z. Xue, S. K. Noh and C. Ba, *Macromolecules*, 2007, **40**, 8600–8608.
33.   Y. Gao, H. Li and X. Wang, *Eur. Polym. J*., 2007, **43**, 1258–1266.
34.   H. M. Li, H. B. Chen, Z. G. Shen and S. Lin, *Polymer*, 2002, **43**, 5455–5461.
35.   P. Ding and B. Qu, *J. of Colloid and Interface Sci*., 2005, **291**, 13–18.

36. L. Qiu, W. Chen and B. Qu, *Colloid. Polym. Sci.,* 2005, **283**, 1241-1245.
37. J. Yang, F. Chen, Y. Ye, Z. Fei and M. Zhong, *Colloid. Polym. Sci.*, 2010, **288**, 761-767.
38. S. Lv, W. Zhou, H. Miao, and W Shi, *Prog Org Coat.*, 2009, **65**, 450–456.
39. S. Ozgumus, M. K. Gök, A. Bal and G. *Güçlü, Chem. Eng. J.,* 2013, **223**, 277–286.
40. L. Wang, S. Shengpei, D, Chen and C.A Wilkie, Polym. *Degrad. Stabil.,* 2009, **94**, 770-774.
41. K. Chibwe and W. Jones, J. Chem. Soc., *Chem. Commun.*, 1989, **14**, 926-927.
42. T.A. Saleh, *App. Surf. Science*, 2011, 257, 7746-7751.
43. T.A. Saleh, V.K. Gupta, *Separation and Purification Tech.*, 2012, **89**, 22, 245-251.
44. M. F. Chiang and T. M. Wu, *Compos. Sci. Tech.*, 2010, **70**, 110-115.
45. JCPDS PDF: Powder Diffraction Files; International Centre for Diffraction Data:Newtown Square, PA, 1977.
46. W. Cui, Q. Jiao, Y. Zhao, H. Li, H. Liu and M. Zhou, *eXPRESS Polym. Lett,* 2012, **6**, 485-489.
47. Y. Bao, Z. Huang and Z. Weng, *J. App. Polym. Sci.*, 2006, **102**, 1471-1477.
48. M. Jaymand, *Polym. J.,* 2011, **43**, 186-193.
49. S. J. Palmer and R. L. Frost, *Coord. Chem. Rev.,* 2009, **253**, 250–267.
50. N. H. Huang and J. Q. Wang, *eXPRESS Polym. Lett.,* 2009, **3**, 595-604
51. K. Kristina, P. Igoris, T. Ricardas, K. Alexander and K. Aivaras, *Cent. Eur. J. Chem.*, 2011, **9**, 275-282.
52. F. Malherbe and J. Besse, *J. Solid State Chem.*, 2000, **155**, 332–341. 332–341.
53. F. Picchioni, E. Passaglia, G. Ruggeri and F. Ciardelli, *Macromol. Chem. Phys.,* 2001, **202**, 2142–2147.
54. J. Liu, G. Chen and J. Yang, *Polymer*, 2008, **49**, 3923-3927.
55. F. Cavani, F. Trifiró and A. Vaccari, *Catal. Today.*, 1991, **11**, 173-301.